Journal of Statistical Physics, Vol. 76, Nos. 1/2, 1994

Self-Consistent Check of the Validity of Gibbs Calculus Using Dynamical Variables

Dominique Escande,[1] Holger Kantz,[2] Roberto Livi,[3] and Stefano Ruffo[4]

Received October 1, 1993; final February 16, 1994

The high- and low-energy limits of a chain of coupled rotators are integrable and correspond respectively to a set of free rotators and to a chain of harmonic oscillators. For intermediate values of the energy, numerical calculations show the agreement of finite time averages of physical observables with their Gibbsian estimate. The boundaries between the two integrable limits and the statistical domain are analytically computed using the Gibbsian estimates of dynamical observables. For large energies the geometry of nonlinear resonances enables the definition of relevant 1.5-degree-of-freedom approximations of the dynamics. They provide resonance overlap parameters whose Gibbsian probability distribution may be computed. Requiring the support of this distribution to be right above the large-scale stochasticity threshold of the 1.5-degree-of-freedom dynamics yields the boundary at the large-energy limit. At the low-energy limit, the boundary is shown to correspond to the energy where the specific heat departs from that of the corresponding harmonic chain.

KEY WORDS: Gibbs ensembles; coupled rotators; resonance overlap; large-scale chaos; relaxation to equilibrium.

1. INTRODUCTION

A key question in statistical physics is to know when time averages of physical observables agree with statistical averages performed in the suitable

[1] Equipe Turbulence Plasma de l'URA 773, CNRS, Université de Provence, Institut Mediterranéen de Technologie, Château-Gombert, F-13451 Marseille, France, and DRFC, Centre d'Etudes de Cadarache, 13108 Saint Paul lez Durance Cedex, France.

[2] Fachbereich Physik, Bergische Universität—Gesamthochschule Wuppertal Gauss, Strasse 20, D-42097 Wuppertal 1, Germany.

[3] Dipartimento di Fisica, Università di Bologna, and INFN and INFM, 2, I-40126 Bologna, Italy.

[4] Dipartimento di Energetica, Università di Firenze, I-50123, Firenze, and INFN and INFM, Sezione di Firenze, Italy.

0022-4715/94/0700-0605$07.00/0

ensemble. Moreover, in many applications (e.g., in molecular dynamics simulations[1]) one needs a fast relaxation in time with a limited number of degrees of freedom. From the point of view of the theory of dynamical systems this corresponds to knowing what degree of chaos is needed to enable a generic orbit to sweep sufficiently the phase space in a short time ("large-scale" chaos). This is a very difficult question to establish in high-dimensional Hamiltonian systems.

Quite recently, numerical simulations were devoted to exploring this problem, controlling at the same time the degree of chaos through the measurement of the spectrum of Lyapunov exponents. No conclusive result was reached on the delimitation of the region of agreement between time and *ensemble* averages.[2] In order to make some progress, it is necessary to choose an appropriate model for which the knowledge of the geometrical properties of the phase space can be pushed as far as to understand the onset of "large-scale" chaos. To this end we have chosen a model of nearest-neighbor coupled rotators on a 1D lattice.[3]

Following the path opened by Nekhoroshev and Chirikov[4] in the geometry of resonances, we have introduced a low-dimensional approximating Hamiltonian for this model, which turns out to describe quite well some low-dimensional aspects of the high-dimensional motion at large and intermediate energies. This Hamiltonian leads us to introduce an appropriate overlap parameter which enables us to delimit from above the energy region where *ensemble* averages of some physical observables agree with time averages. More precisely, one can compute the probability distribution of the overlap parameter in the canonical ensemble and determine, in a statistical sense, the upper energy boundary of the region of "large-scale" chaos using a simple Chirikov overlap criterion combined with a canonical ensemble calculation. The lower-energy boundary can be estimated by a heuristic reasoning involving the onset of nonlinear effects.

In Section 2 we introduce the model, show the result of the calculations of equilibrium energy density and specific heat, and compare these results with those obtained from time averages. In Section 3 we present a qualitative description of the dynamics of the perturbed pendula which constitute the chain of rotators. Section 4 is the core of the paper; here we present in detail the canonical transformation which permits the selection of the low-dimensional aspects of our high-dimensional system. Section 5 is devoted to the numerical investigation of the effect of clustering of local resonances. In Section 6 we obtain the main result of this paper by computing the probability distribution of the overlap parameter. In Section 7 we present some conclusions and perspectives for future investigations.

2. THE MODEL, GIBBS AVERAGES, AND TIME AVERAGES

Let us consider the Hamiltonian

$$H = \sum_{i=1}^{N} \left\{ \frac{p_i^2}{2} + [1 - \cos(q_{i+1} - q_i)] \right\} = K + U \tag{2.1}$$

with periodic boundary conditions

$$q_1 = q_{N+1}, \qquad p_1 = p_{N+1} \tag{2.2}$$

K and U stand for the kinetic and potential parts of H, respectively. In all the simulations the total momentum of the chain is set to zero for to both prevent center-of-mass motion and agree with the assumptions of our Gibbs calculations.

The Hamiltonian (2.1) describes the motion of a system of N coupled rotators and can be thought of as describing the nontrivial conservative dynamics of a one-dimensional XY model. Dissipative Langevin dynamics and Monte Carlo dynamics are known to relax rapidly to statistical equilibrium in one dimension, while conservative dynamics like (2.1) are generally not ergodic.

We introduce Gibbs averages through the canonical partition function

$$Z = \int \prod_i dq_i \, dp_i \, e^{-\beta H} \tag{2.3}$$

where β is the inverse temperature $\beta = T^{-1}$ and the Boltzmann constant $k_B = 1$. Livi *et al.*[2] showed how to perform the calculation of the average potential energy density $\bar{U}$ and of the specific heat at constant volume C_V. We recall here only the result of this calculation:

$$\begin{aligned} \bar{U} &= 1 - \frac{I_1(\beta)}{I_0(\beta)} \\ C_V &= \frac{1}{2} + \beta^2 \left[1 - \frac{1}{\beta} \frac{I_1(\beta)}{I_0(\beta)} - \left(\frac{I_1(\beta)}{I_0(\beta)} \right)^2 \right] \end{aligned} \tag{2.4}$$

where I_0, I_1 are modified Bessel functions. The results in formulas (2.4) are independent of the *ensemble* in the thermodynamic $N \to \infty$ limit; in particular, they stay the same in the microcanonical ensemble. Finite-N corrections can be computed[2] and are generally negligible for the N values we use in numerical simulations.

Time averages are instead naturally performed in the microcanonical

ensemble for conservative systems. A time-dependent temperature $T(t)$ is defined through the average kinetic energy

$$T(t) \equiv 2 \frac{\langle K \rangle}{N} \tag{2.5}$$

where the symbol $\langle \cdot \rangle$ stands for the finite time average $\langle \cdot \rangle \equiv (t)^{-1} \int_0^t \cdot \, dt'$. Analogously one defines the average potential energy $\langle U \rangle / N$. The time-dependent specific heat at constant volume $\tilde{C}_V(t)$ is given by the fluctuations of the kinetic energy[5]

$$\tilde{C}_V(t) \equiv \frac{1}{2} \left(1 - \frac{N}{2} \frac{\langle K^2 \rangle - \langle K \rangle^2}{\langle K \rangle^2} \right)^{-1} \tag{2.6}$$

In ref. 2 the specific heat was computed from the total energy fluctuations of a small part of the chain, mimicking a canonical ensemble calculation. This latter method is affected by larger fluctuations and we have preferred here the definition (2.6). In principle, the two methods cannot give the same result if the system is not ergodic.

These quantities should agree with canonical averages [Eq. (2.4)] after the double limit N, $t \to \infty$ is performed. This limit is impossible to realize in numerical simulations; therefore one is interested to know for which values of N and t one obtains a good agreement with canonical

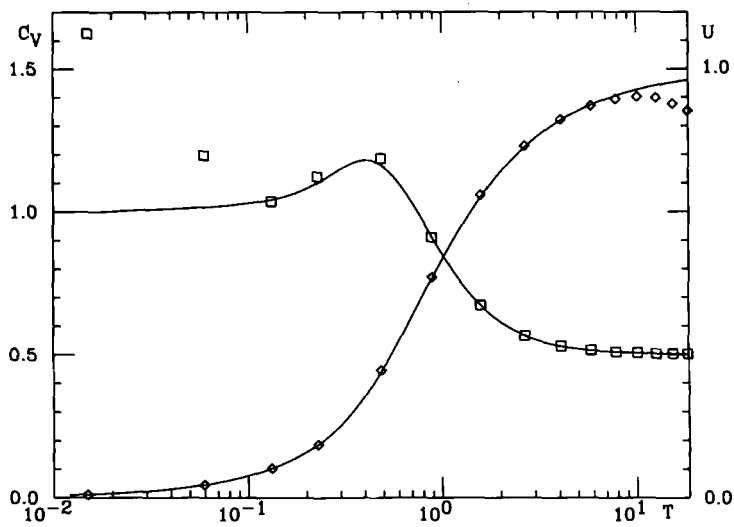

Fig. 1. Plot of C_V and $\langle U \rangle$ vs. T. Numerical estimates: C_V (□) and $\langle U \rangle$ (◇); Gibbsian predictions (—).

averages. For the model under examination the value of N is not crucial: one obtains a good agreement over a large intermediate temperature region ($0.1 < T < 10$) for moderate values of N, $N \sim 100$. This is an indication that a *statistical regime* exists. In Fig. 1 we report the result of canonical and time averages of the internal energy and of the specific heat for $N = 128$ as a function of T at $t = 35{,}000$. Statistical fluctuations are of the size of the symbols in Fig. 1, but a slow relaxation is present at large and small temperatures. Increasing N does not improve significantly the result at small and large temperatures.

3. RELAXATION AND DYNAMICS

A crucial role in the qualitative description of the motion is played by the temperature T. It is proportional to the energy density H/N (an exact relation can be found which links the two quantities at equilibrium[6]), and appears obviously in all the formulas concerning Gibbs averages, but it is also a natural control parameter for the characterization of the motion. If $T \gg 1$, then $\langle K \rangle \gg \langle U \rangle$ and the rotators decouple and move freely. Hence, we define the *weak-coupling regime* by the condition $T \gg 1$. On the contrary if $T \ll 1$ the kinetic energy is not enough to excite large-amplitude motion of the rotators and we are therefore in the limit of almost linearly coupled oscillators. We call this limit the *strong-coupling regime*. In both limits our model is nearly integrable, although the action–angle Hamiltonian is different in the two limits (quadratic in the actions at large temperature and linear at small temperatures). This makes the analysis quite different.

Coming back to the reproduction of Gibbs averages, it is clear that it is exactly in these two limits that relaxation is slow. In fact, the time needed to reach the *ensemble* average becomes very large in the small- and large-temperature regions. More precisely, the specific heat $\tilde{C}_V(t)$ shows a slow relaxation in time at temperatures T below the boundary to the strong-coupling region, which is placed at $T_s \approx 0.1$. The internal energy badly converges at temperatures larger than $T_w \approx 10$; they both show a fast relaxation at intermediate temperatures (the subscripts w and s indicating the weak- and strong-coupling limits, respectively). For small T the agreement with the Gibbsian estimate of the average potential energy derives trivially from the linear virial theorem. Analogously for large T the kinetic energy has small relative fluctuations, which imply the Gibbsian value 0.5 for the specific heat. In Fig. 2 we show the convergence time t_x of $\tilde{C}_V(t)$ and of $\langle U \rangle / N$ to within x percent of the Gibbsian estimate for several values of x. The convergence time changes significantly in the vicinity of T_s and T_w. In the following we discuss the dynamical explanation of the good convergence of physical observables in the *statistical regime*, i.e., $T_w > T > T_s$,

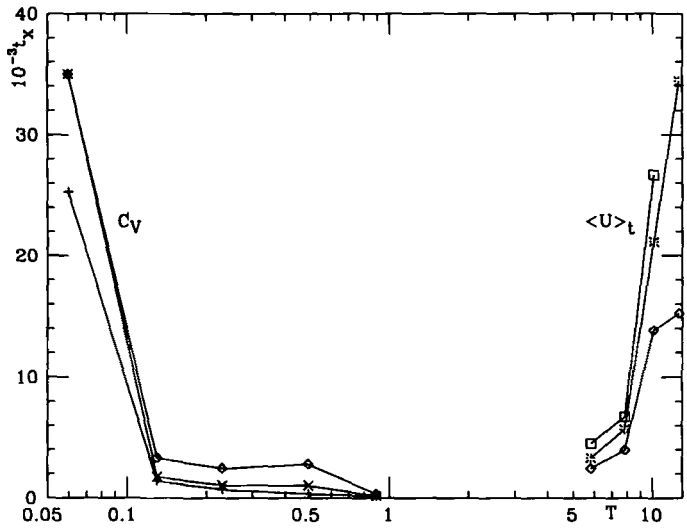

Fig. 2. Plot of first time t_x when the numerical estimates of C_V ($T<1$) and $\langle U \rangle_t$ ($T>5$) reach the Gibbsian prediction up to an x% error: $x=20\%$ (+), $x=10\%$ (×), $x=5\%$ (◇), $x=3\%$ (*), $x=2\%$ (□). The upper point to the left is a lower bound.

and show that a Gibbsian calculation predicts the existence of the boundary temperatures T_w and T_s.

Let us introduce the following variables for a fixed pair of rotators:

$$I_1 = \frac{p_{i+1} - p_i}{\sqrt{2}}$$
$$\Psi_1 = \frac{q_{i+1} - q_i}{\sqrt{2}} \tag{3.1}$$

whose appropriate meaning and relevance will become clear in the following. Numerical simulations performed with random initial conditions show that an orbit in the restricted phase space $S_1 \equiv (\Psi_1 (\mathrm{mod}\, 2\sqrt{2}\,\pi), I_1)$, of each pair of neighboring rotators may result in a libration inside a "separatrix," a rotation outside it, or an alternation of rotation and libration during time evolution, depending on the temperature. These are typical situations for a perturbed pendulum. Some typical orbits in S_1 are reported in Fig. 3. We can distinguish three different regimes from numerical simulation:

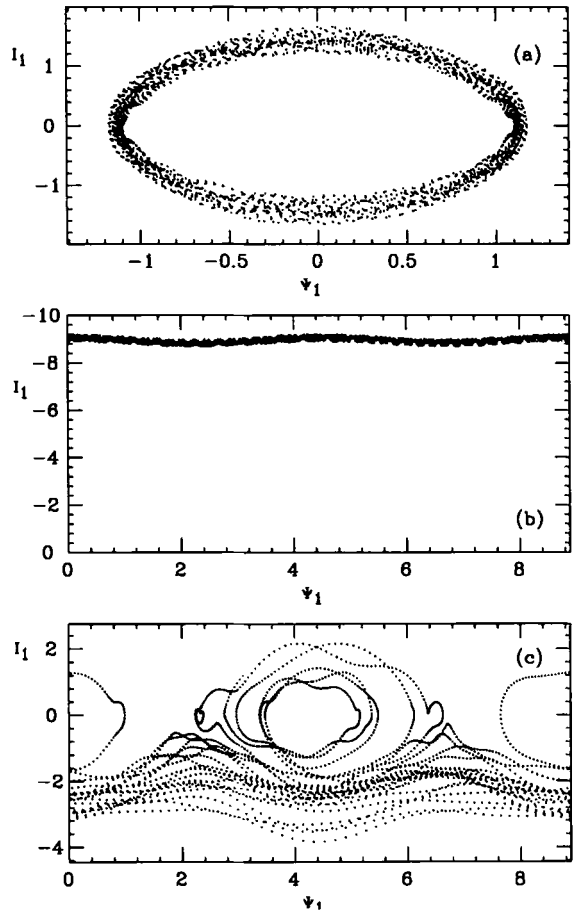

Fig. 3. Typical librating (a), rotating (b), and separatrix crossing (c) orbits in the restricted phase plane S_1. We plotted 2500 points stroboscopically at fixed time intervals $\Delta t = 0.05$ for $N = 16$, $T \sim 61.1$ [(a) and (b) correspond to two different pairs of the same run], and $T \sim 5.2$ [part (c)]. The separatrix width is 2 and in (c) the orbit was started outside of it. The spread of the points is mainly an effect caused by the stroboscopic view.

• *Weak-coupling regime* $T \gg 1$. Each pair of rotators remains either in rotation or in libration for a very long time; "separatrix" crossing is very rare. The system is frozen in the initial state.

• *Statistical regime* $T_s < T < T_w$. The restricted phase space of each pair shows alternation in time of rotation and libration; "separatrix" crossing is frequent and happens more or less randomly in time.

• *Strong-coupling regime* $T \ll 1$. Each pair goes in libration inside the "separatrix" for any initial condition.

Below we shall call a pair *active* if its motion is a libration in S_1. The approximation that we develop in the following enables us to interpret this result and to obtain a precise definition of what up to now we have loosely called "separatrix." In particular, starting from the observation that in the *weak-coupling regime* it is natural to single out a series of pendula (primary resonances)[4, 7] related to the N cosines of Hamiltonian (1.1), it is possible to obtain an approximating time-dependent Hamiltonian which describes the motion of a pair of rotators on a finite time span.

4. THE RESONANCE FRAME

It is our aim to find an appropriate canonical change of variables which separates slow from fast motion and reduces the effective number of relevant degrees of freedom. More precisely, our goal is to reduce the complexity of the motion to that of a single perturbed pendulum, which is the typical feature of the dynamics we observe in S_1.

It is clear that to reach this result the relevant canonical coordinates are the differences in angles $(q_{i+1} - q_i)$. To obtain some hints on the construction of the canonical transformation that we have to perform let us consider the integrable case of two rotators, i.e., the Hamiltonian

$$H = \frac{p_1^2 + p_2^2}{2} - \cos(q_1 - q_2) \tag{4.1}$$

There are in this case two degrees of freedom and two constants of motion in involution: the Hamiltonian itself and the total momentum $P = p_1 + p_2$. Thus, the model is integrable and we can isolate the single resonance from the fast free motion. In the weak-coupling limit the constant-energy E surface is a circle of radius $(2E)^{1/2}$ in the (p_1, p_2) plane: the resonance line $p_1 = p_2$ is the bisectrix of the first quadrant. To isolate the "pendulum" Hamiltonian we follow a geometric idea. We perform a pseudorotation (in fact a unitary transformation with determinant -1) by $\pi/4$ of the (p_1, p_2) reference frame and a shift of its origin by the average momentum $p_* = (p_1 + p_2)/2$ in order to represent the sphere in the new action coordinates $\mathbf{I} = (I_1, I_2)$ as a paraboloid which, in the I_1 direction, has a functional representation beginning with a quadratic term. The new angles $\boldsymbol{\Psi} = (\Psi_1, \Psi_2)$ are defined by the same pseudorotation. Thus

$$\begin{aligned} p_1 &= p_* + (I_2 - I_1)/\sqrt{2} \\ p_2 &= p_* + (I_2 + I_1)/\sqrt{2} \\ \Psi_1 &= (q_2 - q_1)/\sqrt{2} \\ \Psi_2 &= (q_2 + q_1)/\sqrt{2} \end{aligned} \tag{4.2}$$

It is easy to verify that this is a canonical transformation with generating function

$$F(\mathbf{I}, \mathbf{q}) = p_*(q_1 + q_2) + \frac{1}{\sqrt{2}}\left[I_1(q_2 - q_1) + I_2(q_2 + q_1)\right] \tag{4.3}$$

and the new Hamiltonian is

$$H = H_1 + H_2 \tag{4.4}$$

with

$$\begin{aligned} H_1(I_1, \Psi_1) &= I_1^2/2 - \cos(\sqrt{2}\,\Psi_1) \\ H_2(I_2) &= p_*^2 + \sqrt{2}\,p_* I_2 + I_2^2/2 \end{aligned} \tag{4.5}$$

H_1 corresponds to a pendulum whose phase space display a "cat's eye," the signature of a nonlinear resonance. H_2 is separately integrable since it depends only on actions. Thus

$$\begin{aligned} \Psi_2(t) &= \sqrt{2}\,p_* t + I_2(0) \\ I_2(t) &= I_2(0) \end{aligned} \tag{4.6}$$

represents a fast free motion.

For higher dimensions ($N \geqslant 3$) Hamiltonian (1.1) is no longer integrable. The primary resonance conditions $p_j = p_{j+1}$ define a net of hyperplanes which intersect the unperturbed energy hypersphere in action coordinates in the weak-coupling limit, thus leading to a much more complex situation. However, we may try to retain the geometrical image that we got from the two-dimensional case and define a direction orthogonal to the hypersphere living on the hyperplane $p_{j+1} = p_j$ of the jth primary resonance and study the motion close to this resonance, i.e., we choose a pair of rotators satisfying the resonance condition. Since the hypersphere is locally a hyperparaboloid, it is the new angle variable Ψ_2 conjugated to the new action I_2 defined along this direction which develops fast motion, and will play the role of time in our approximating Hamiltonian. In the hyperplane of codimension one orthogonal to this direction an "eye of cat" will open,

but now the phase of the cosine will in general depend on all degrees of freedom. Hence, we have to choose our unitary $N \times N$ matrix representing the pseudorotation in order to minimize the influences of the other degrees of freedom. In the following we give a first recipe for the construction of this matrix.

We perform the following canonical transformation:

$$(\mathbf{p}, \mathbf{q}) \to (\mathbf{I}, \boldsymbol{\Psi}) \tag{4.7}$$

whose generating function is[4]

$$F(\mathbf{I}, \mathbf{q}) = \sum_i \left(p_i^{(r)} + \sum_k I_k \mu_{ki} \right) q_i = (\mathbf{p}^{(r)} + \mathbf{I}\hat{\mu})\mathbf{q} \tag{4.8}$$

where the row "resonance" vector $\mathbf{p}^{(r)}$ defining the direction orthogonal to the unperturbed energy hypersphere (and whose squared modulus is of the order of the unperturbed energy) and the matrix $\hat{\mu}$ have to be chosen in an appropriate way. We do not expect the approximate Hamiltonian to remain valid for all times. Therefore we define a sequence of times $(\tau_1, \tau_2, ..., \tau_n, ...)$ at which we fix both $\mathbf{p}^{(r)}(\tau_n)$ and $\hat{\mu}(\tau_n)$, and thus the canonical transformation, by the rule we give in the following. The approximating Hamiltonian $H(t, \tau_n)$ will be used in the time interval $[\tau_n, \tau_{n+1}]$ and the rule for passing from $H(t, \tau_n)$ to $H(t, \tau_{n+1})$ will also be given.

The change of variables defined by the canonical transformation (4.8) is

$$\mathbf{p} = \frac{\partial F}{\partial \mathbf{q}} = \mathbf{p}^{(r)} + \mathbf{I}\hat{\mu}$$

$$\boldsymbol{\Psi} = \frac{\partial F}{\partial \mathbf{I}} = \hat{\mu}\mathbf{q} \tag{4.9}$$

We have first to define the resonance vector. Let us consider the momentum vector $\mathbf{p}$ at the fixed time τ_n; then $\mathbf{p}^{(r)}$ is defined as

$$\mathbf{p}^{(r)} = (p_1(\tau_n), p_2(\tau_n), ..., p_{j-1}(\tau_n), p_*, p_*, p_{j+2}(\tau_n), ..., p_N(\tau_n)) \tag{4.10}$$

where the average momentum (no longer conserved) is

$$p_* = \frac{p_{j+1}(\tau_n) + p_j(\tau_n)}{2} \tag{4.11}$$

For the matrix $\hat{\mu}$ we require the following properties:

- $\hat{\mu}$ is unitary.
- Let $\mathbf{R}_k$ be the set of orthonormal row vectors of $\hat{\mu}$; then one of these vectors is defined in terms of $\mathbf{p}^{(r)}$,

$$\mathbf{R}_2 = (0,..., 0, p_{j-1}(\tau_n), p_*, p_*, p_{j+2}(\tau_n), 0,..., 0)/\mathcal{N} \tag{4.12}$$

where

$$\mathcal{N} = [p_{j-1}^2(\tau_n) + 2p_*^2 + p_{j+2}^2(\tau_n)]^{1/2} \tag{4.13}$$

Equations (4.10)–(4.13) define completely what we call the "resonance frame" depending on the time τ_n at which it is fixed.

The choice (4.12) can be justified by the following argument. In the statistical regime, the (I_1, Ψ_1) dynamics looks numerically quite similar to that of a pendulum perturbed by a time-dependent potential: chaotic "separatrix" crossings occur, and are presumably related to the existence of stochastic layers close to resonance hyperplanes. The origin of this low-dimensional behavior may be suspected to stem from nearby resonances, i.e., from resonances produced by the cosines with arguments where q_j and q_{j+1} are present. Hamiltonian (1.1) has only two such resonances: those with indices $j-1$ and $j+1$ (encompassing four degrees of freedom from $j-1$ to $j+2$). Thus we account only for these resonances and this leads to definition (4.12). In the case where $p_{j+1}(\tau_n) = p_j(\tau_n)$, $\mathbf{R}_2$ is the projection of the normal to the unperturbed energy surface onto the momentum subspace with indices $i = j-1,..., j+2$.

We are now left with the choice of the other row vectors $\{\mathbf{R}_k, k \neq 2\}$.

A natural form for a normalized row vector orthogonal to $\mathbf{p}^{(r)}$ is the following:

$$\mathbf{R}_1 = \left(0,..., -\frac{1}{\sqrt{2}}, \frac{1}{\sqrt{2}},..., 0\right) \tag{4.14}$$

where the jth and $(j+1)$th components only are nonzero and opposite. This implies

$$\begin{aligned} \Psi_1(t) &= \mathbf{R}_1 \cdot \mathbf{q} = \frac{q_{j+1}(t) - q_j(t)}{\sqrt{2}} \\ \Psi_2(t, \tau_n) &= \mathbf{R}_2 \cdot \mathbf{q} \end{aligned} \tag{4.15}$$

Moreover,

$$I_1(t) = \frac{p_{j+1}(t) - p_j(t)}{\sqrt{2}}$$
$$I_2(t, \tau_n) = [\mathbf{p}(t) - \mathbf{p}^{(r)}] \cdot \mathbf{R}_2 \tag{4.16}$$

Let us observe that $I_2(\tau_n, \tau_n) = 0$.

After making explicit the canonical transformation for the angles one obtains the following Hamiltonian in terms of the new variables $(\mathbf{I}, \mathbf{\Psi})$:

$$\begin{aligned} H(t, \tau_n) = H_1 + \frac{|\mathbf{p}^{(r)}|^2}{2} + \frac{1}{2} I_2^2 + \mathcal{N} I_2 \\ - \cos\left[-\frac{\Psi_1(t)}{\sqrt{2}} + \omega_+(\tau_n)\, \Psi_2(t, \tau_n) + \rho_+(t, \tau_n) \right] \\ - \cos\left[-\frac{\Psi_1(t)}{\sqrt{2}} + \omega_-(\tau_n)\, \Psi_2(t, \tau_n) + \rho_-(t, \tau_n) \right] \\ + \mathcal{H}' \end{aligned} \tag{4.17}$$

with H_1 given in (4.5) and where

$$\begin{aligned} \rho_+(t, \tau_n) &= q_{j+2} - q_{j+1} + \frac{\Psi_1(t)}{\sqrt{2}} - \omega_+(\tau_n) \Psi_2 \\ \rho_-(t, \tau_n) &= q_j - q_{j-1} + \frac{\Psi_1(t)}{\sqrt{2}} - \omega_-(\tau_n) \Psi_2 \end{aligned} \tag{4.18}$$

and

$$\begin{aligned} \omega_+(\tau_n) &= R_{2,j+2} - R_{2,j+1} \\ \omega_-(\tau_n) &= R_{2,j} - R_{2,j-1} \end{aligned} \tag{4.19}$$

The residual Hamiltonian $\mathcal{H}'$ does not depend on Ψ_1, I_1, and I_2. Thus the dynamics in this restricted phase space S_1 does not depend on the other degrees of freedom. Hamiltonian (4.17) describes a 1.5-degree-of-freedom system. It has the form of the three-wave "paradigm" Hamiltonian[7]; one can recognize the primary resonance of H_1 and two side primary resonances. The pendulum phase space (Ψ_1, I_1) is coupled to the other variables through Ψ_2 and the "rests" ρ_+ and ρ_-. The low-dimensional description of the motion is appropriate if Ψ_2 grows linearly and the "rests" remain constant. From the Hamiltonian (4.17) this is true if I_2 remains small with respect to $\mathcal{N}$; then Ψ_2 is the fast "time" variable which drives the diffusion

in the actions. Moreover, for infinite temperature, i.e., zero coupling, the phase space is foliated by unperturbed tori, and replacing the solution $q_i(t) = p_i(0)t + q_i(0)$ in (4.18), one obtains $\rho_{\pm} = 0$ after straightforward calculations. Obviously, in the weak-coupling region $\rho_{\pm}$ remains small.

We performed numerical simulations at $T \gg 1$ to verify that this picture is correct at least in the weak-coupling regime. The results are displayed in Fig. 4 for $T \sim 30.2$, $N = 16$, and confirm the validity of the low-dimensional representation of the motion: $\Psi_2 \sim \mathcal{N} \cdot t$ ($\mathcal{N} \sim 2.08$) and the "rests" remain almost constant with respect to the growth of Ψ_2 on appreciable durations, while I_2 fluctuates about a value which is much smaller than $\mathcal{N}$.

In the statistical regime Ψ_2 starts to grow linearly, but, at a certain moment, when $|I_2|$ becomes of the order of $\mathcal{N}$, it stops its linear growth. This is the warning that the resonance frame fixed at τ_n is no longer appropriate. The change of dynamical regime of Ψ_2 is due to the effect of side resonances, which drive the change in p_{j-1} and p_{j+2}, that in the end produces an increase of I_2. This intricate effect could have been analytically computed only if we had taken into account a set of three resonances (four rotators) in the approximating Hamiltonian, which would have been a higher-order approximation than that of Hamiltonian (4.17). Therefore, we have verified in numerical experiments the simultaneous saturation of the

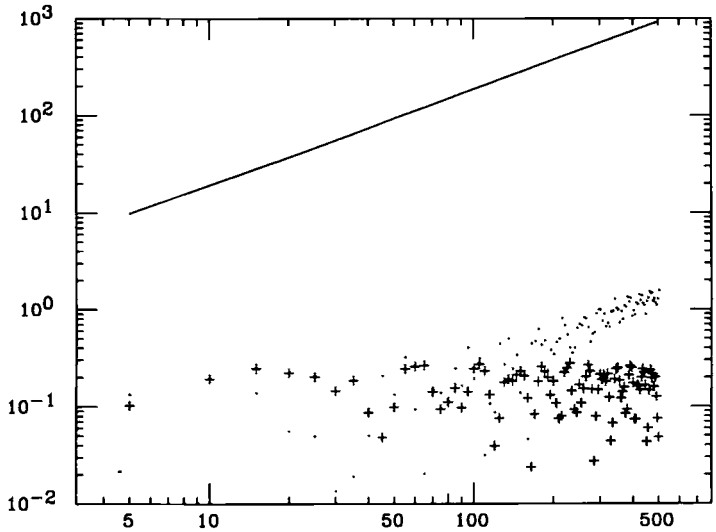

Fig. 4. Plots of Ψ_2 (solid line), $|\rho_+|$ (dots), and $|I_2|$ (crosses) versus time in the *weak-coupling regime.*

linear growth of Ψ_2 in correspondence with the increase of I_2; this always happens when $|I_2|$ reaches a significant fraction of $\mathcal{N}$. Thus, we have to establish a heuristic criterion for the change to a new approximating Hamiltonian of the form (4.17). Empirically, we change the frame when $|I_2| = 0.5 \times \mathcal{N}$; this defines τ_{n+1}. The new approximating Hamiltonian $H(t, \tau_{n+1})$ is consequently defined by the new canonical transformation in terms of the new values of $\mathbf{p}^{(r)}$ and $\hat{\mu}$ at time τ_{n+1}. We have also checked that changing by some 10–20% the criterion does not change significantly the results. When this is done we recover large sections of linear growth of Ψ_2 and constancy of the "rests" during the motion (see Fig. 5). This suggests the validity of the approximating Hamiltonian (4.17) also in the statistical regime.

Trapping in either of the nonlinear resonances related to the two cosines of Eq. (4.17) was also observed in numerical experiments, looking at the cylindric phase space $(I_1, \bar{\Psi}_1)$ with $\bar{\Psi}_1 = \Psi_1 - \sqrt{2}\,\omega_+ \Psi_2 - \sqrt{2}\,\rho_+$ for the +-resonance. To this end we must choose an initial condition inside the side resonance; this requires $d\Psi_1/dt(0) = \sqrt{2}\,\omega_+ |\mathcal{N}|$. Assuming that the "rest" ρ_+ is constant, this is equivalent to imposing $p_{j+1} = p_{j+2}$. This is also trivially equivalent to representing the motion in the frame of the side resonance. After this is done, bounded motion inside the +-resonance is easily detected.

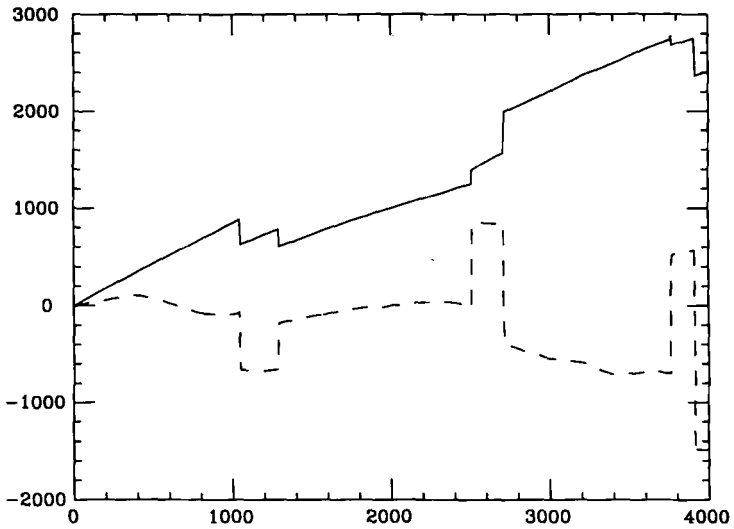

Fig. 5. Plots of Ψ_2 (full line) and ρ_+ (broken line) versus time for $T = 7.32$, i.e., in the *statistical regime*. The abrupt discontinuities shown by the two curves correspond to the times τ_n when the resonance frame is changed; this is done when $I_2 = 0.5\mathcal{N}$.

5. CLUSTERS OF RESONANCES

Since the Hamiltonian $H(t, \tau_n)$ gives a good description of the low-dimensional aspects of the dynamics generated by (1.1) in the weak-coupling limit, one can use the expression for the separatrix given by Hamiltonian H_1 to detect when a resonance may be active. We define the mean activity parameter A as

$$A = \frac{\sum_j (\text{time resonance } j \text{ is active})}{(\text{total time}) \times N} \tag{5.1}$$

and the crossing rate χ as the mean number of separatrix crossings per unit time. In Fig. 6 we show both A and χ as functions of T, averaged over eight random initial conditions for $N = 8$ (it has been shown in numerical simulations[8] that both these parameters are independent of N). When T is large the probability that a pair of rotators is in resonance is small and furthermore the energy transfer among the rotators is negligible. Thus A and χ are small. Decreasing the temperature below $T \approx 10$, one observes an increase of both A and χ, indicating the onset of large-scale chaos. The

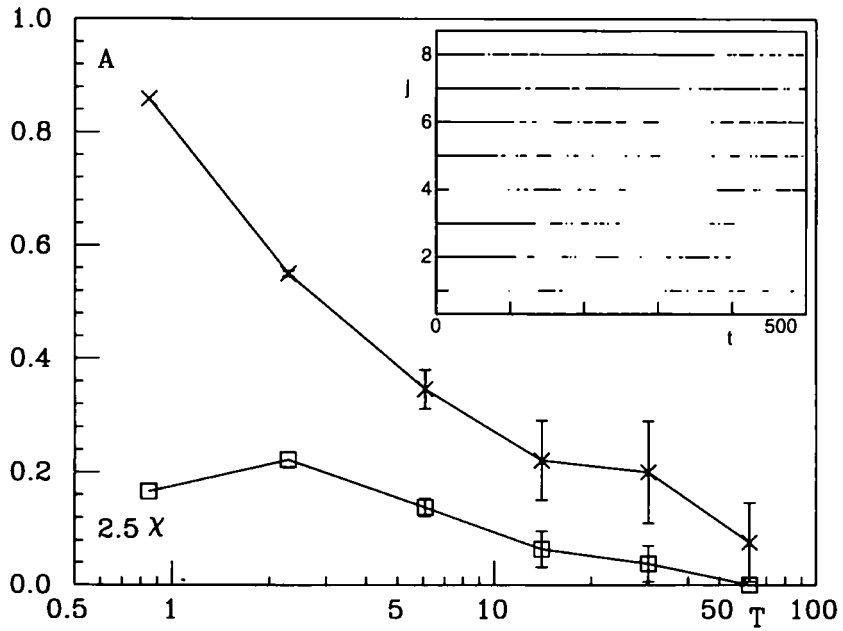

Fig. 6. Plot of the activity A and crossing rate χ versus temperature. The error bars indicate the variance over the eight initial conditions. The inset shows the labels of active resonances versus time.

Gibbs calculation of A is also feasible and shows the same behavior as the one reported in Fig. 6.[6,8]

In the inset of Fig. 6 we plot the labels of active resonances versus time during a run for $T=3.5$: the frequent switching of the trajectory from one resonance to another or its simultaneous presence in two nearby resonances makes explicit the dynamical mechanism responsible for the existence of large-scale chaos. It is also evident from the inset, and even clearer if one performs simulations with larger values of N, that clusters of more than two active resonances may form in the *statistical regime*. This effect should be taken into account in the approximating Hamiltonian, but for the study of the transition from the *weak-coupling* to the *statistical regime* it is enough to restrict consideration to an approximation containing only one central resonance, such as the one leading to the Hamiltonian $H(t, \tau_n)$.

This is further confirmed by the fact that the formation of the clusters of different sizes is a statistical phenomenon, regulated by the dynamics of each resonant pair of rotators. This is easily seen if one measures the probability distribution $P(l)$ of clusters of size l of active resonances normalized to the number of time steps and of rotators. As shown in Fig. 7, this is an exponential function $P(l) \simeq e^{-Sl}$ for various values of T in the *statistical regime* and the slope of the exponential S is very close to $-\ln A$. The continuous curves in Fig. 7 represent the theoretical formula $P(l) = A^l(1-A)^2$,

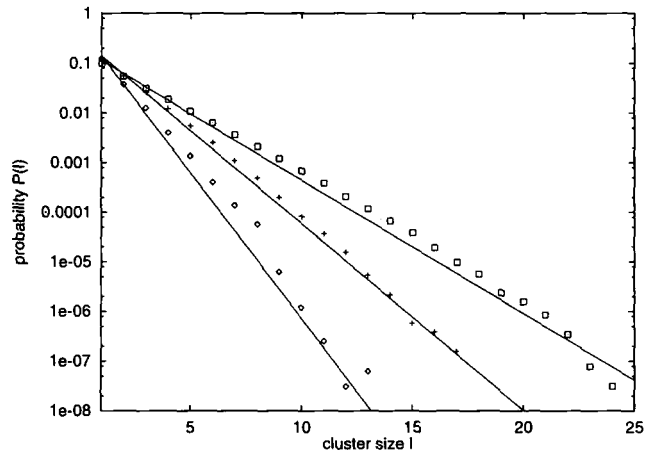

Fig. 7. Probability distribution $P(l)$ for clusters of active resonances size l versus the cluster size for various temperatures T in the statistical regime: (□) $T=3.07$, $A=0.539$; (×) $T=5.57$, $A=0.421$; (◇) $T=10.72$, $A=0.258$. Here A is the activity parameter defined in formula (5.1). For comparison we plot $(1-A)^2 A^l$ in all three cases (—).

where the factor $(1-A)^2$ takes into account the inactive resonances at the borders of a cluster of active resonances. Thus, we guess that the exponential behavior for large l is a consequence of the cluster formation being a Poisson independent process, essentially due to an independent visit of the resonances.

6. BOUNDS OF THE STATISTICAL REGIME

As observed above, the dynamics described by Hamiltonian (4.17) is that of a 1.5-degree-of-freedom system. In such a system, chaotic orbits flow from the primary resonance (H_1) to side resonances after the breakup of the last KAM torus. Chaotic transport directly connects close primary resonances. Before this breakup, diffusion in phase space is much slower and occurs through the thin stochastic layers of the Arnold web[9] formed by higher-order resonances. It is natural to expect that the temperature T_w corresponds to the transition to the large-scale chaotic regime. No estimate of the breakup threshold of the full three-resonance Hamiltonian (4.17) is available. Hence, we have followed the treatment of ref. 7, where the two-resonance Hamiltonian is studied in detail, and we have used the results contained there to estimate the breakup threshold, neglecting the effect of one of the side resonances. Therefore we introduce the overlap parameter

$$s_{\pm} = \frac{4}{\omega_{\pm} \mathcal{N}} \tag{6.1}$$

It is the ratio of the width of the unperturbed separatrix to the distance of the side ($\pm$) resonances. In the naive Chirikov treatment the transition to the large-scale chaotic regime occurs at resonance overlap, i.e., $|s_{\pm}| \sim 1$; this value has been refined by a renormalization group treatment for the "paradigm" two-resonance Hamiltonian to $s_{\pm}^{\text{trans}} \sim 0.7$.[7]

In our high-degree-of-freedom system the overlap parameters are expected to have a statistical distribution $\mathcal{P}(s_{\pm})$ in the statistical regime. This is trivially not true if we perform a numerical simulation in the weak-coupling regime; here the distribution of overlap values is frozen close to the initial state. However, since the overlap parameters defined in (6.1) depend only on momenta, if we fix the initial condition according to a Maxwellian distribution of momenta, the overlap distribution remains fixed in time. Hence, both in the statistical and in the weak-coupling regimes a canonical ensemble calculation of the overlap distribution is meaningful from two different points of view; in the former case any distribution of overlap relaxes to the equilibrium one, in the latter the initial equilibrium overlap distribution is conserved in time. Thus, we present here the calcula-

tion of the overlap distribution in the canonical ensemble. From (6.1) the overlap parameter is a function only of momenta p_i. Moreover, the partition function of model (1.1) is the product of two independent factors, depending on momenta and coordinates separately, $Z = Z_p Z_q$, with

$$Z_p = \left(\frac{2\pi}{\beta}\right)^{N/2} \tag{6.2}$$

The calculation of the probability distribution of the overlap parameter is better performed after a simple change of variables. Let us perform the calculation for s_+. One first observes that the inverse v_+ of s_+ is a linear function of the momenta

$$v_+ = \frac{1}{s_+} = \frac{2p_{j+2} - p_{j+1} - p_j}{8} \tag{6.3}$$

Therefore one can integrate the partition function (6.2) over the momenta which do not appear in v_+ and, by a change of variables introducing v_+, one rewrites Eq. (6.2) in the following form:

$$\frac{1}{4}\left(\frac{2\pi}{\beta}\right)^{3/2} = \int dp_j\, dp_{j+1}\, dv_+ \exp -\frac{\beta}{2}\left[p_j^2 + p_{j+1}^2 + \frac{1}{4}(8v_+ + p_j + p_{j+1})^2\right] \tag{6.4}$$

The integration over p_j, p_{j+1} leads to the probability distribution of v_+, from which we obtain $\mathscr{P}(s_+)$

$$\mathscr{P}(s_+) = \frac{\mathscr{K}}{s_+^2} \exp -\left(\frac{16\beta}{3s_+^2}\right) \tag{6.5}$$

where $\mathscr{K} = (16\beta/3\pi)^{1/2}$ is the normalization factor. As for other canonical averages, $\mathscr{P}$ depends only on $\beta = T^{-1}$. The maximum of the distribution is at

$$s_{\max} = \left(\frac{16}{3T}\right)^{1/2} \tag{6.6}$$

$\mathscr{P}$ is shown in Fig. 8 for $s_+ > 0$ and three different values of T. When compared with numerical results for $T = 2.9$ (a value inside the *statistical regime*) which starts from a nonequilibrium initial condition (momenta are uniformly distributed in a finite interval and all coordinates are set to zero), not only is the qualitative behavior of $\mathscr{P}$ confirmed but, surprisingly enough, the agreement is also quantitatively good in view of the adopted

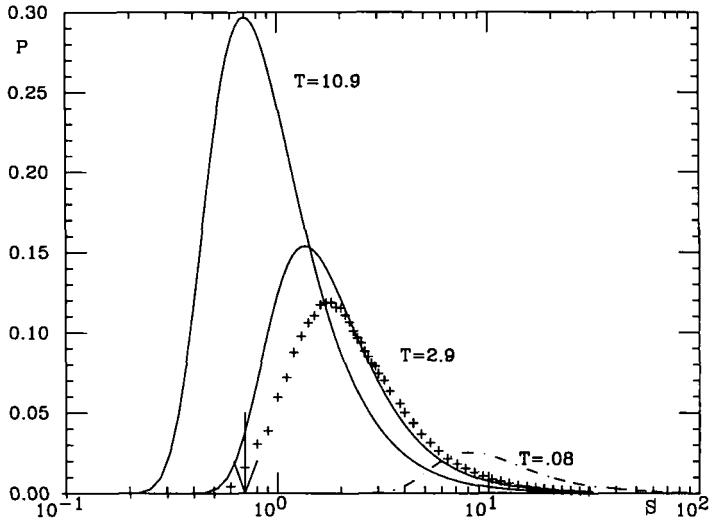

Fig. 8. Plot of $P(s)$ versus s for $T=10.9$, $T=2.9$, and $T=0.08$; $s=0.7$ is indicated by an arrow. The crosses result from a numerical simulation performed at $T\sim 2.9$.

approximations in the analytical prediction. As we increase the temperature from the statistical regime, the most probable overlap decreases, although still some fraction of resonances have a significant overlap. This is in agreement with the numerical observation that the system becomes less and less chaotic as the temperature increases. On the contrary, for smaller values of T the overlap is large on the average and one therefore observes large-scale chaotic motion. A rough estimate of the upper bound of the statistical regime is obtained requiring that the maximum of the distribution $s_{\max}$ equals s_{+}^{trans}. This gives $T_{\text{trans}}\sim 10.9$, which is close to the upper bound of the *statistical regime*. The estimate of this upper bound strongly depends on the form of the Hamiltonian (4.17) and its validity is a convincing indirect confirmation of the approximating dynamics given by Hamiltonian (4.17). Although this estimate of T_{trans} is based on the evaluation of the overlap distribution in the statistical regime, one may be doubtful about it because we extend the reasoning to the transition region between the statistical regime and the weak-coupled regime, where the canonical distribution is not expected to be valid. However, as we already remarked, we expect that in this transition region an initial canonical momentum distribution is invariant in time. Therefore, we may interpret the statistical distribution $\mathscr{P}(s_{\pm})$ as obtained from averaging over an ensemble of systems which are initially distributed according to a Maxwellian distribution of momenta, and then extend the validity of our analysis into the

weak-coupling regime. Of course, we are here extending a nonequilibrium reasoning which implies relaxation to equilibrium to a region that does not present it, but this is intrinsic to any attempt to analyze the transition to large-scale chaos in many-dimensional systems.

Using formula (6.5), it is also easy to estimate the chaotic fraction F of the phase-space as a function of temperature T, under the assumption that one can consider the global phase space as a product of subspaces corresponding to each resonance. Indeed, after a change of variables, we have

$$F = \frac{2}{\sqrt{\pi}} \int_0^{s_{\max}/s_{\pm}^{\text{trans}}} e^{-x^2}\, dx = \operatorname{erf}\left(\left[\frac{16}{3T(s_{\pm}^{\text{trans}})^2} \right]^{1/2} \right) \tag{6.7}$$

It is a slowly decreasing function of T, which also follows quite well the dependence of the activity A on the temperature T in Fig. 6. Its value is still quite high at the weak-coupling boundary, of the order of 80%, but the curve $F(T)$ has an inflection point at T_w, detecting a fast increase of the chaotic fraction of the phase space up to the boundary of the statistical regime followed by a saturation of the same quantity inside the statistical regime.

The strong-coupling boundary T_s has a simple dynamical justification. Since we know that large-scale chaos sets in as we lower the energy (temperature) from the weak-coupling regime, we expect to reach the same chaotic regime as we increase the energy from the strong-coupling regime. Indeed, the onset of large-scale chaos occurs when the nonlinearity of the force between rotators comes into play and induces chaotic energy exchanges among the vibrational eigenmodes [recall that model (1.1) is nonintegrable so that other kinds of nonlinear phenomena, such as exact solitons, are excluded]. This happens for values of the energy well below the one of the separatrix of H_1; it is the well-known energy of the transition to equipartition seen in anharmonic oscillators.[10] This chaos happens as a consequence of the same mechanism of resonance overlap described for the weak-coupling side, but about a different and much more complex quasi-integrable limit, involving an integrable Hamiltonian which is linear in the action (thus making questionable even the applicability of the KAM theorem).[11]

However, we can use again an argument based on Gibbs averages to get an estimate of T_s. In fact, the nonlinearity of the force also affects the Gibbsian estimate of the specific heat $C_V(T)$ and makes it depart from the harmonic equipartition law $C_V(T) = 1$ around $T = 0.1$. The boundary temperature T_s, as indicated by the deviation of the Gibbsian $C_V(T)$ from its low-temperature limit, can be estimated as the intersection of the tangent

of the left inflection point of $C_V(T)$ versus T in linear scale with the line $C_V(T)=1$. This yields $T\approx 0.08$, which is close to the estimate of T_s obtained from the time relaxation properties of the specific heat $\bar{C}_V(T)$ (see Fig. 2). The transition to the *strong-coupling* limit may also be understood from the point of view of the approximating Hamiltonian (4.17). Indeed, this limit corresponds to a strong resonance overlap induced by a very slow time dependence of (4.17). In this regime chaos becomes quite slow and inefficient.[12] We have therefore been able to delimit the region of agreement between *ensemble* and time averages using Gibbsian averages of appropriate dynamical observables.

7. CONCLUSION

This paper has made one step toward deriving statistical mechanics from classical mechanics by using concepts from the theory of chaos. Namely it provided a way for Gibbsian theory to check its validity self-consistently in a model of coupled rotators. For such a model the high- and low-energy limits are integrable, but there is a sizable range of energy where finite time averages of observables agree with their Gibbsian estimates. The boundary temperatures between the statistical and the two integrable domains were computed using Gibbsian tools on dynamical observables. In particular, for the high-energy boundary the geometry of nonlinear resonances enabled the derivation of a new observable, the resonance overlap parameter of appropriate 1.5-degree-of-freedom Hamiltonian systems.

Several directions are opened for future work. On this model, the use of chaotic transport theory could help in providing estimates of the minimum time necessary for the convergence of time averages. This model is characterized by a near-neighbor coupling, but a nonlocal interaction in angle space. Other models of coupled rotators may be investigated:

- A mean-field model of globally coupled rotators with the same force[13] which is similar to a one-dimensional plasma.
- A near-neighbor model with local interaction.
- A mean-field model of globally coupled rotators which would be reminiscent of the Boltzmann gas.

ACKNOWLEDGMENTS

The collaboration which led to this paper was made possible thanks to financial support from the Université de Provence, the Instituto Nazionale di Fisica Nucleare, and the Università di Firenze. H. K. thanks the European Community for partial financial support. We thank the Institute

for Scientific Interchange in Torino for hospitality during the workshops Complexity and Evolution 1991 and 1992 and their participants for useful discussions. We thank, moreover, Yves Elskens for many useful discussions and constructive criticism. We finally thank CINECA for the use of CPU time on the CRAY-YMP under the grant G4WFIZQ1.

REFERENCES

1. G. Ciccotti and W. G. Hoover, eds., *Molecular Dynamics Simulation of Statistical-Mechanical Systems* (North-Holland, Amsterdam, 1986); G. Ciccotti, D. Frenkel, and I. R. McDonald, eds., *Simulation of Liquids and Solids* (North-Holland, Amsterdam, 1987).
2. R. Livi, M. Pettini, S. Ruffo, and A. Vulpiani, *J. Stat. Phys.* **48**:539 (1987).
3. G. Benettin, L. Galgani, and A. Giorgilli, *Nuovo Cimento B* **89**:89, 103 (1985).
4. B. V. Chirikov, *Phys. Rep.* **52**:263 (1979).
5. J. L. Lebowitz, J. K. Percus, and L. Verlet, *Phys. Rev.* **153**:250 (1967).
6. Y. Elskens, private communication.
7. D. F. Escande, *Phys. Rep.* **121**:166 (1985).
8. B. Peters, Memoire de Maitrise, Université de Provence, Marseille (1992).
9. V. I. Arnol'd, *Dokl. Akad. Nauk SSSR* **156**:9 (1964); L. Chierchia and G. Gallavotti, Drift and diffusion in phase space, CARR Report 15/92 (1992).
10. H. Kantz, R. Livi, and S. Ruffo, *J. Stat. Phys.* **76**:627(1994).
11. A. J. Lichtenberg and M. A. Lieberman, *Regular and Chaotic Dynamics* (Springer, 1992, Chapter 6.5b, pp. 443ff.
12. C. R. Menyuk, *Phys. Rev. A* **31**:3282 (1985); Y. Elskens and D. F. Escande, *Physica D* **62**:66 (1992).
13. S. Ruffo, Hamiltonian dynamics and phase transitions, in *Transport, Chaos and Plasma Physics* (World Scientific, Singapore, 1994).